

# Design of a Haptic Device with Variable Stiffness Actuation Mechanism for Finger Rehabilitation

Arash Basirat Tabrizi<sup>1</sup>, Jeremy Catania<sup>1</sup>, Baiqian Qi<sup>2</sup>, Kouros Zareinia<sup>1</sup>

<sup>1</sup>Toronto Metropolitan University, Department of Mechanical, Industrial and Mechatronics Engineering  
350 Victoria Street, Toronto, ON, Canada

[abasirat@torontomu.ca](mailto:abasirat@torontomu.ca); [jcatania@torontomu.ca](mailto:jcatania@torontomu.ca); [kouros.zareinia@torontomu.ca](mailto:kouros.zareinia@torontomu.ca)

<sup>2</sup>The University of Hong Kong, Biomedical Engineering Programme  
Pokfulam, Hong Kong, China

[baiqianq@connect.hku.hk](mailto:baiqianq@connect.hku.hk)

**Abstract** – To address the limitations of existing actuation mechanisms for end-effector hand rehabilitation devices, this study presents an electro-mechanical, variable stiffness, actuation mechanism. The proposed solution best suits the task of active-resistive rehabilitation treatment of fingers. The miniature design enables a large range of motion, real-time input control, and exerts continuous resistive forces of up to 5 Newtons on the user’s fingertip. A finger-sized end-effector haptic device assembled using off-the-shelf components and 3D printed parts helps realize the mechanism. The implemented actuator can operate at a maximum stroke of 36 mm. Furthermore, experimental measurements of the mechanism’s force profile are a good match with simulation predictions. The powered device is safe, easy to store, operate, and assemble.

**Keywords:** Haptic device, Hand rehabilitation device, Linear actuator, Voice coil actuator, Variable Stiffness

## 1. Introduction

Over the past five years Canada has witnessed a significant economic commitment, with \$2.86 billion dedicated solely to Physical Rehabilitation Nursing Units (PRNU) [1]. These specialized units cater to inpatients with stable disabilities, focusing on restoring or enhancing functional abilities through comprehensive programs. Notably, an average of 75% of admitted inpatients were senior citizens aged 65 and above [2], reflecting a significant demographic trend. The economic impact is underscored by a median hospital stay of 22 days [3], highlighting the prolonged resource allocation to rehabilitation services within hospitals.

Amidst the users of PRNU, individuals grappling with the aftermath of stroke and spinal cord injuries (SCI) face substantial challenges in performing activities of daily living (ADLs) [4], [5]. For instance, weakness in the muscles plays a key role in the decline of motor function in the fingers following a stroke [8]. Research suggests that approximately 85% of individuals affected by stroke globally experience impairment in hand function, with 60% continuing to grapple with upper limb complications, especially in the fingers and wrists, even after receiving treatment and being discharged [7]. Consequently, patients prioritize the recovery of upper-limb functions [6]. Extensive research has demonstrated engaging in activity and exercise as part of rehabilitation therapy is essential for facilitating patients' improvement and aid in their recovery [8].

Rehabilitation therapy encompasses two primary forms: passive, and active [8], [11]. Passive therapy involves no patient effort and is used early post-stroke when there's no response from the limb, often with an assistive rehabilitation robot [11]. Active therapy is for those with some limb movement and includes active-assistive and active-resistive types [11]. Active-assistive involves external force aiding movement, while active-resistive therapy applies opposing force to the fingers [11].

Early rehabilitation management post-stroke or SCI not only enhances patient outcomes but also reduces hospital stays [4]. With hands' vital role in daily activities, hand rehabilitation emerges as crucial for improving quality of life, yet its intensity is constrained by resource availability and therapist presence [4]. To address these challenges, researchers are developing rehabilitation robots as assistive devices, with studies suggesting their efficacy comparable to traditional methods [8]. Powered devices offer a solution to therapy demand, particularly in providing repetitive movements aiding neural pathway development for motor function restoration [8], [11].

Hand rehabilitation devices (HRDs) aim to facilitate hand rehabilitation therapy [8], ideally offering high-intensity training with minimal clinical resources, often in home settings. However, despite increasing HRD development, existing solutions often face complexity in operation and assembly, and struggle with balancing cost and form factor [7]. These devices are typically categorized as orthoses, exoskeletons, or end-effector devices [8]. This research solely concentrates on end-effector HRDs.

Amadeo, a clinically proven end-effector device for hand and finger rehabilitation, produced by Tyromotion GmbH (Steiermark, Graz, Austria) is the most advanced commercial solution for robotic therapy [7], [8]. Amadeo costs up to \$100,000 USD and is sold only to medical institutions [7]. The device's linear rail mechanism enables the actuation of each individual finger, providing active and passive exercises [7], [8]. Other existing hand rehabilitation end-effectors, namely RehaDigit [9] and HandCARE [10], incorporate DC motors and variety of sensors, such as force-sensing resistors (FSRs), to train hand and finger function. The Reha-Digit device uses cylinders to roll the fingers for actuation which enables active and passive stretching of fingers [8], [9]. HandCARE's cable-actuated mechanism assists the subject in opening and closing movements [10]. While both devices are inexpensive compared to Amadeo, they are difficult to assemble, maintain, and have not been commercialized since their introduction in the year 2008.

There are currently no established standards for the development or design of HRDs [8]. Instead, HRDs are identified by their mechanical structures, actuation mechanism, control systems, and therapeutic approaches [8]. This research centers on designing a unique actuation mechanism that addresses the limitations of existing solutions.

## **2. Problem Statement**

This study presents the design and implementation of a variable stiffness actuation mechanism for the purpose of finger rehabilitation. The variable stiffness mechanism allows users to configure the device according to their individual needs, providing a singular solution for varying injury severity and abilities. To this extent, an end-effector device will be assembled to demonstrate the mechanism. The device is tailored for a miniaturized design with a size that is comparable to the human finger. The end-effector must enable planar movement of a finger. End-effector designs prioritize actuation at the distal interphalangeal (DIP) finger joint rather than the entire finger [8]. The device must be stationary to keep the hand steady during rehabilitation exercises. Moreover, the device should be user-friendly, safe, and simple to assemble. Off-the-shelf components are preferred for the assembly to reduce implementation cost. The proposed mechanism is intended for active-resistive rehabilitation treatment and should generate resistive forces of up to 5 Newtons.

## **3. Actuation Mechanism**

Actuation mechanism refers to the mechanism utilized in devices to convert power transmitted from actuators within end-effector devices [8]. The most common mechanisms employed by end-effector HRDs are the linkage-based and cable-driven schemes [8]. Linkage-based actuation employs links, including 3D printed or machined, along with off-the-shelf linear actuators and diverse motors to facilitate powered actuation [8]. While versatile and compatible with various control methods, it's burdened by the added weight and complexity introduced by motors and translational linkages [8].

Cable-driven systems provide an adaptable design that can adjust to the patient's hand dimensions and are considered as low-weight solutions [8]. However, these devices employ servo or brushless DC motors that can be costly with medium to short life cycles [8]. Additionally, cable-driven devices suffer from disadvantages related to loss and control issues. The dependency on cable translation leads to transmission losses during exercise execution, this is exacerbated by friction losses as cables rely on spools for release and retraction, ultimately compromising control [8]. To address the limitations of the existing actuation schemes for hand rehabilitation applications, the following subsections introduce the design and implementation of an electro-mechanical, variable stiffness, actuation mechanism.

### **3.1. Variable Stiffness Mechanism**

The underlying design of the variable stiffness mechanism is inspired by voice coil actuators (VCAs). Originally developed for audio speakers, VCA technology is now a reliable solution for high-precision linear motion control [12]. VCAs benefit from miniature designs, inherit a large motion range, and are suitable for highly repeatable tasks [12], [13].

Furthermore, they have a linear input current and output force relationship and are free from friction and backlash [13]. Moreover, they are back-drivable with minimal resistance, unlike most linear actuators with gear boxes. Figure 1(a) captures the force profile of a high-end commercial VCA [14]. Because of these properties the technology is commonly used in the field of medical robotics [13]. A typical VCA consists of a permanent magnet housed within a movable tubular coil of wire, contained within a ferromagnetic cylinder (Fig. 1(b)). Upon the flow of current through the coil winding, magnetization occurs, leading to repulsion against the magnets and generating reciprocal in-and-out motion. In dynamic use situations the mechanism is able to model second order responses such as based on a mass-spring-damper model.

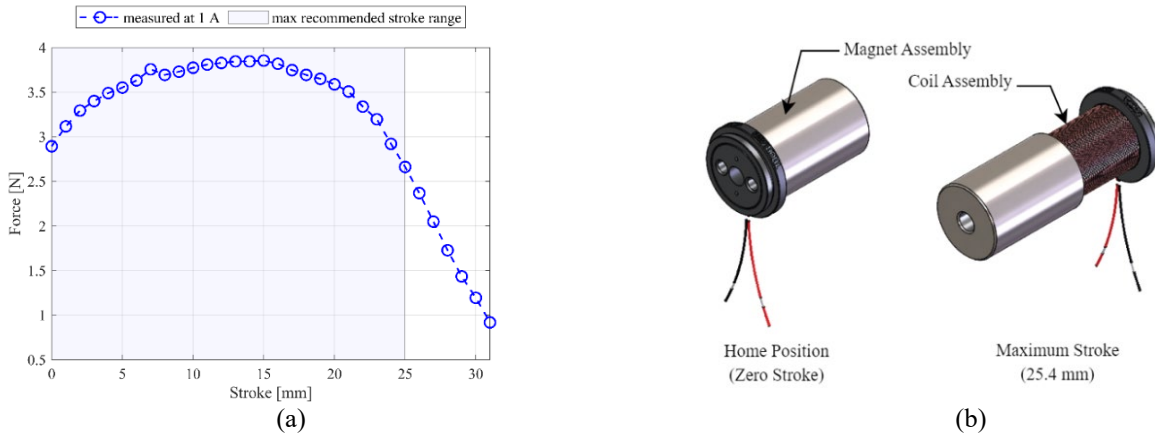


Fig. 1: Thorlabs' VC250 25.4 mm stroke voice coil actuator (a) continuous force profile (b) CAD model.

While commercial VCAs enable accurate bi-directional linear motion control, they are an expensive solution. For example, the VCA from Fig. 1 provides a peak force of approximately 4 Newtons in an operating stroke of 15 mm with a starting price of \$360 USD. The commercial expense of VCAs motivated a design inspired by the conventional VCA and referred to as the variable stiffness actuator (VSA) in this paper. The stiffness is a measure of the resistive force generated by the actuator. Like VCAs, the VSA uses Lorentz force and has a linear force-current profile.

The proposed VSA consists of a neodymium rod permanent magnet (NdFeB N35) and tubular coil assembly. Enamelled magnetic copper wire (21 American Wire Gauge) wrapped around an aluminum double-flange bobbin constructs the coil assembly. Aluminum metals were a favorable design choice for the bobbin because of their paramagnetic properties. The specifications of the off-the-shelf components are captured by Fig. 2.

Given the diameter of the copper wire and the dimensions of the bobbin the parameters in Table 1 are of significance. Assuming ideal packing of the coil winding, the theoretical total number of coil turns,  $n$  (an integer), is calculated from [13]:

$$n = \left\lceil \frac{h_c}{d_c} \right\rceil \left\lceil \frac{2 w_c}{\sqrt{3} d_c} \right\rceil = 872 \quad (1)$$

Table 1: Coil winding parameters.

Parameter	Description
$h_c = 48.6$ mm	Height of coil winding
$w_c = 9.76$ mm	Width of coil winding
$d_c = 0.79248$ mm	Overall coil diameter (with insulation)

Because the permanent magnet and the coil assembly are arranged concentrically, the gap between the coil winding and the magnet is measured to be 3.66 mm. The impact of the design parameters on the force profile of the VSA will be analyzed in Section 4.

### 3.2. Linear Rail Mechanism

To keep the permanent magnet stationary (stator) at a desired location, a combination of an aluminum shaft-support and a 3D printed PLA base were used. A low-profile linear guide rail and two miniature carriages were set up on top of the base to implement the actuation mechanism. Furthermore, a 3D printed PLA housing was used to connect the coil assembly to the carriages. Figure 3(a) illustrates the described setup.

Keeping the permanent magnet stationary while inducing direct constant current in the coil winding generates a magnetic field that interacts with the magnet’s magnetic field. Depending on the direction of the input current the magnetic fields repel or attract each other, causing the coil assembly to actuate. The actuation is realized because of the linear rail mechanism. The actuator’s stroke parameter measures the amount of finger displacement from its home position.

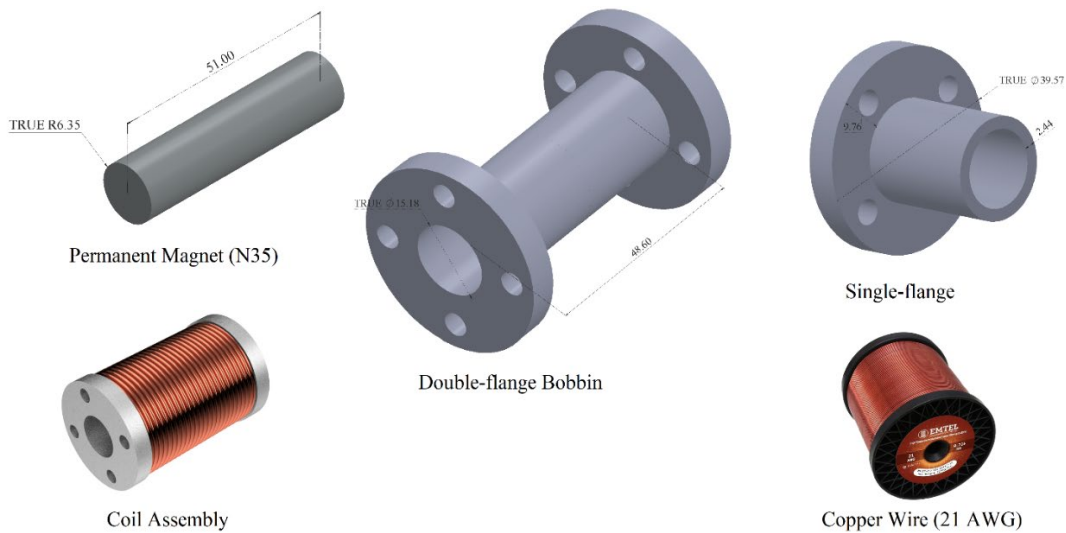


Fig. 2: Off-the-shelf assembly components (all dimensions in mm).

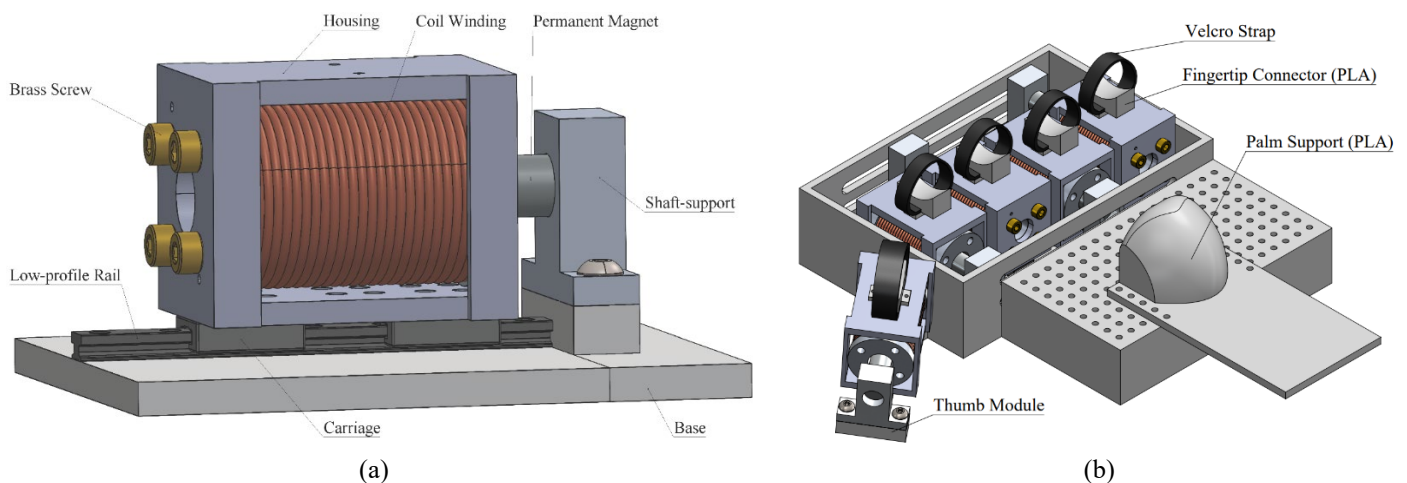


Fig. 3: (a) CAD model of VSA prototype (b) CAD model of HRD (inside view, under development).

#### 4. Numerical Results and Parametric Study

The performance of the VSA was analyzed using the magnetostatic solver of ANSYS Maxwell 3D simulation package. At the home position (Fig. 4(b)) 36.39 mm of the magnet was covered by the coil assembly. Figure 4(a) captures the linear force-current relationship of the actuator measured at the home position. Increasing the total number of coil turns leads to a higher peak force, as indicated by the results. The VSA inherits a continuous-force profile, highlighted by the dashed lines of Fig. 4(a), however, the parametric sweep was executed for select input current values to speed up the simulation.

Additionally, a position sweep simulation was carried out to investigate the force experienced by the moving coil assembly at different operating strokes. The results are captured by Fig. 5(a) and resemble the force profile of the commercial VCA discussed earlier (see Fig. 1(a)). A peak force of approximately 4.93 Newtons in an operating stroke of 12 mm (Fig. 5(b)) was recorded for constant input current of 3 A.

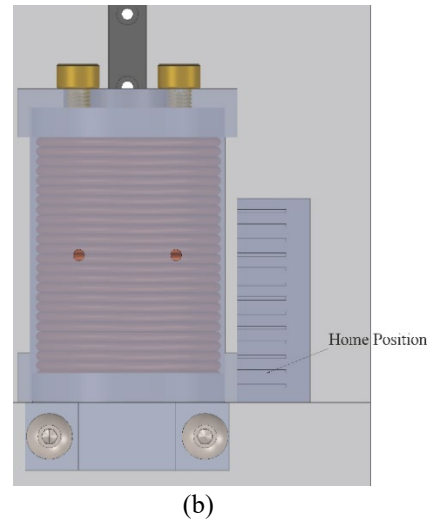
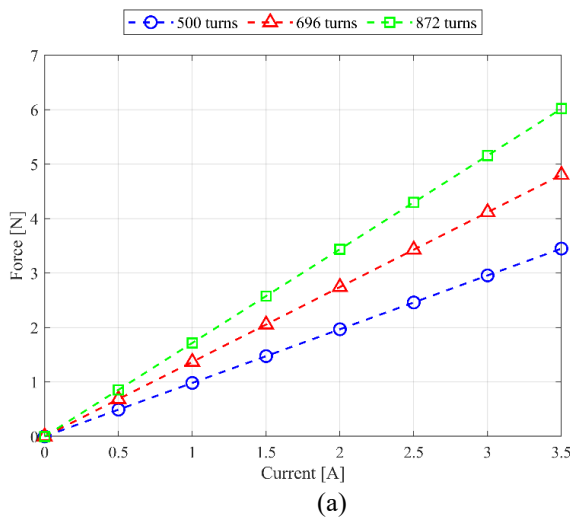


Fig. 4: (a) input current and output force relationship numerical measurements at home position (b) CAD model of VSA's home position (zero stroke).

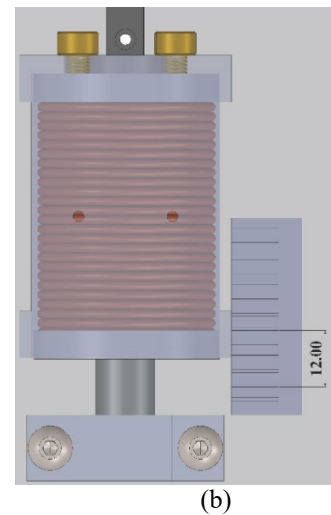
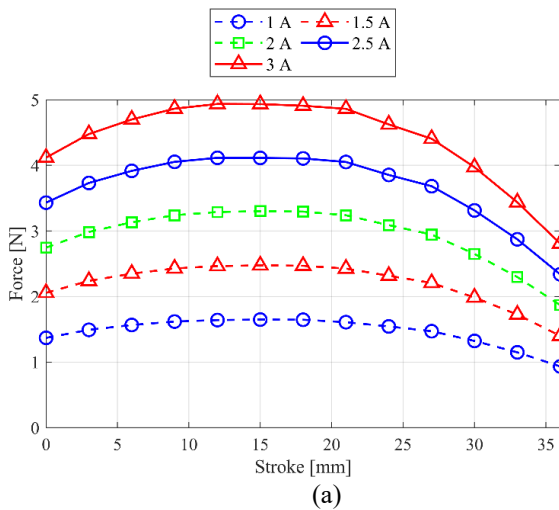


Fig. 5: (a) moving coil numerical measurements for 696 turns (b) CAD model of VSA operating at 12 mm stroke.

## 5. Fabrication and Experimental Results

To assemble the setup shown in Fig. 3(a), the base and the housing were 3D printed first. The copper wire was wrapped around the bobbin and the total number of coil turns were recorded using a planetary gear motor's hall effect with a resolution of 103.8 PPR at the output shaft. The bobbin was mounted to the housing with brass screws. The was screwed to the carriages and the linear rail was screwed to the base. The physical assembly is captured by Fig. 6(a). Table 2 summarises the final design parameters of the VSA.

Table 2: Final design parameters.

Parameter	Value
Weight of coil assembly	0.239 kg
Total number of coil turns	696
Resistance of winding	3.3 $\Omega$
Maximum operating current	3.0 A
Maximum stroke	36 mm
Gap between magnet and coil	3.66 mm

The total resistance of the coil winding was measured by an LCR meter. The maximum stroke and gap parameters were measured using a digital caliper and verified with the measurements extracted from the CAD model. To measure the performance of the VSA, the physical assembly was clamped to a desk and a digital force gauge was used to record forces at different operating strokes. Figure 6(b) illustrates this setup. The system was powered using a custom built 4-channel current regulator ( $V_{MAX} = 12$  V) that interacted with QUANSER's 8-channel USB data acquisition board (Fig. 7(a)) through MATLAB's Simulink environment. QUANSER's real-time control (QUARC) Simulink toolbox enabled precise real-time manipulation of the VSA's input current. Figure 7(b) captures the Simulink model used for real-time input current control.

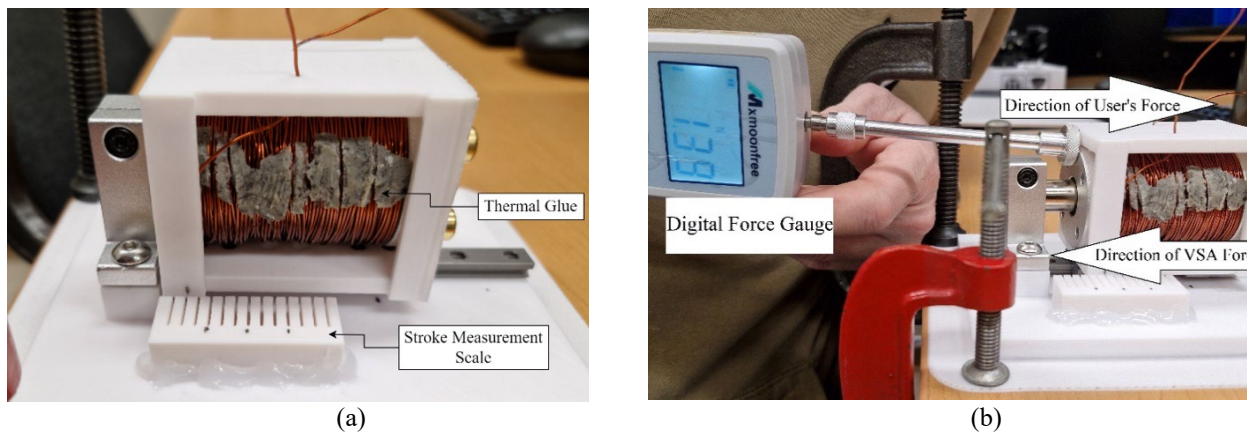


Fig. 6: (a) physical end-effector assembly (b) experimental measurement setup.

The performance of the experimental setup is captured by Fig. 8. The results suggest that the force profile is in good agreement with the numerical results. Each data point in Fig. 8(a) represents the average of five experimental trials. Furthermore, a digital IR laser thermometer was used to record the temperature profile captured by Fig. 8(b). Coil assemblies with two configurations, 500 and 696 coil turns respectively, were fabricated; however, only the latter configuration was

used in the final prototype. Temperature readings for each configuration were conducted on different days to accommodate system cooldown.

A peak force of approximately 4.7 Newtons in an operating stroke of 12 mm was measured for constant input current of 3 A. The primary factors contributing to the 0.2 Newtons peak force difference between numerical and experimental measurements are the manual wrapping of the coil winding, the minimal friction between the carriages and the linear rail, and the human error introduced while using the force gauge. A peak temperature of 33.7 °C was recorded at the top surface of the housing after five minutes of operation. This is a safe operating temperature for the user and the PLA material, and the end-effector is not expected to be powered for longer than a few minutes during rehabilitation exercises.

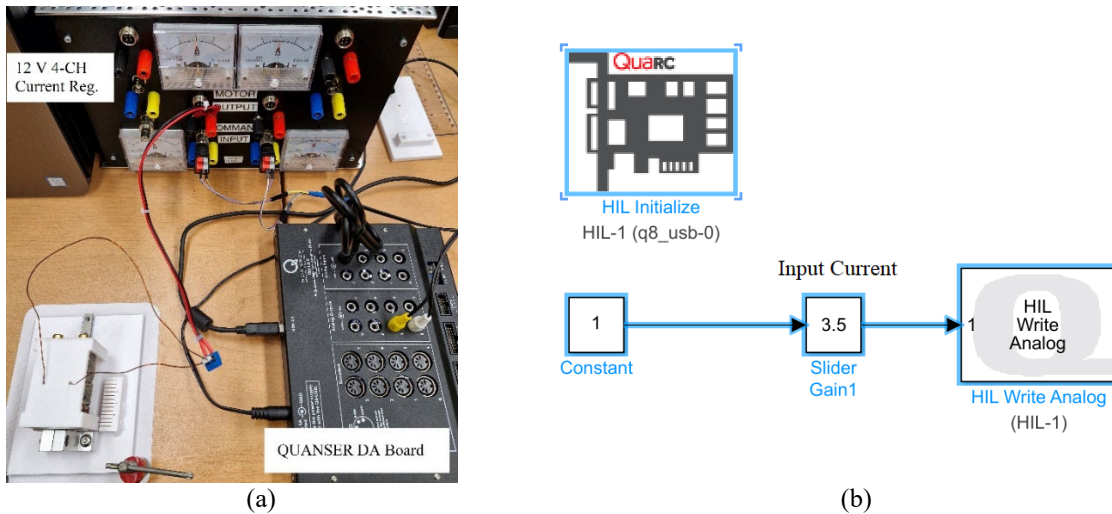


Fig. 7: (a) experimental setup power electronics (b) real-time current controller Simulink interface.

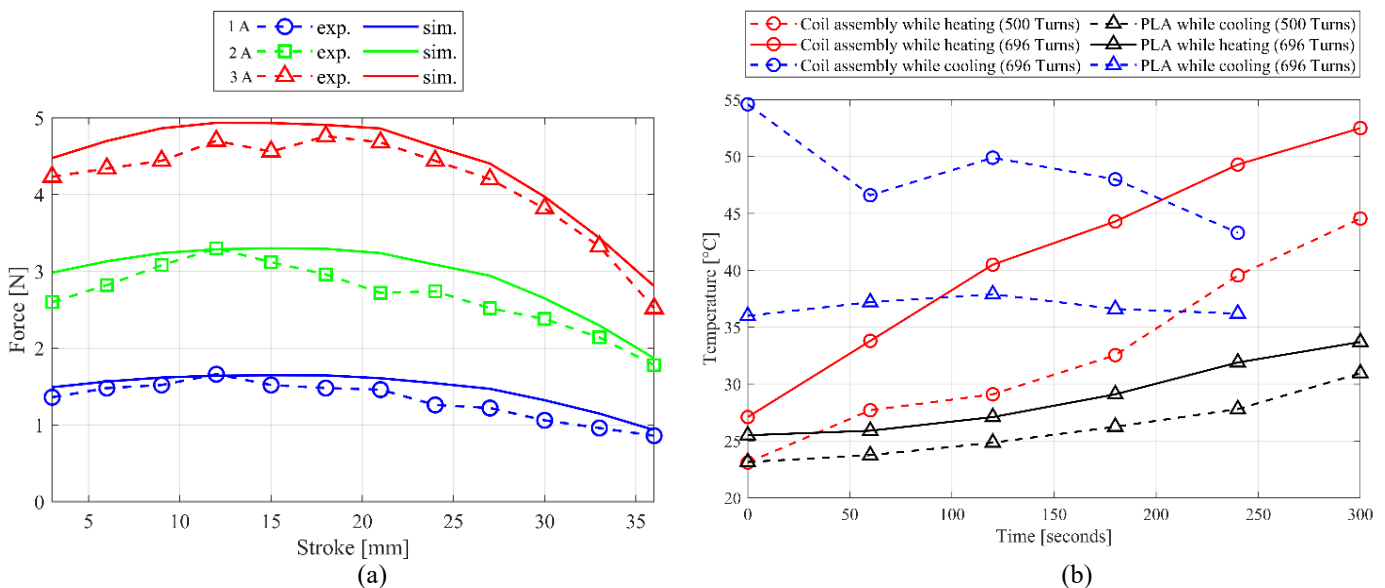


Fig. 8: (a) moving coil exp. measurements comparison with numerical (sim.) results for 696 coil turns (b) temperature profile at constant input current of 3 A.

## 4. Conclusion and Future Work

This research introduced a unique variable stiffness actuation mechanism for the purpose of finger rehabilitation. The proposed electro-mechanical design addressed the limitations of existing end-effector actuation mechanisms for hand rehabilitation applications. The haptic device can perform highly repeatable tasks and exert resistive forces on the user's finger. The end-effector is safe, easy to store and operate, and can be easily assembled using off-the-shelf components and low-cost 3D fabrications. The finger-sized VSA was realized using a linear rail mechanism and generated forces up to 5 Newtons for constant input current of 3 A. Additionally, the miniature design enabled a maximum stroke of 36 mm. The large range of planar motion suits users with different finger sizes.

To enhance the design's performance, utilizing an automatic CNC coil winder machine can increase force output without altering the device dimension. Furthermore, a more robust and accurate measurement setup can be implemented to remove the human element during force readings. In the future, we will integrate multiple VSA modules within a single system to develop and test an affordable and portable HRD. Figure 3(b) presents a visualization of this prototype. The proposed HRD is expected to provide active-resistive rehabilitation exercises for five fingers independently and simultaneously.

## References

- [1] Canadian Institute for Health Information, Canadian MIS Database (CMDB), "Trends in hospital spending, series-C data tables," Accessed Nov 17, 2023.
- [2] Canadian Institute for Health Information, Canadian MIS Database (CMDB), "Demographic characteristics of inpatient rehabilitation clients," Accessed Nov 2023.
- [3] Canadian Institute for Health Information, Canadian MIS Database (CMDB), "Median length of stay in inpatient rehabilitation," Accessed Nov 2023.
- [4] Y. Liu, and C. Yeow, "A portable soft hand exerciser with variable elastic resistance for rehabilitation and strengthening of finger, wrist, and hand," *ASME. J. Med. Devices*, Sep 2015.
- [5] X. Chen, F. Liu, Z. Yan, S. Cheng, X. Liu, H. Li and Z. Li, "Therapeutic effects of sensory input training on motor function rehabilitation after stroke," *Medicine (Baltimore)*, Nov 2018.
- [6] R. J. Visée, J. Likitlersuang and J. Zariffa, "An effective and efficient method for detecting hands in egocentric videos for rehabilitation applications," *IEEE Transactions on Neural Systems and Rehabilitation Engineering*, vol. 28, no. 3, pp. 748-755, Mar 2020.
- [7] B. Sheng, J. Zhao, Y. Zhang, S. Xie and J. Tao, "Commercial device-based hand rehabilitation systems for stroke patients: State of the art and future prospects," *Heliyon*, Feb 2023.
- [8] R. Kabir, M.S.H Sunny, H.U. Ahmed and M.H. Rahman, "Hand Rehabilitation Devices: A Comprehensive Systematic Review," *Micromachines*, 2022. 13(7): p. 1033.
- [9] S. Hesse, H. Kuhlmann, J. Wilk, C. Tomelleri and S.G.B Kirker, "A New Electromechanical Trainer for Sensorimotor Rehabilitation of Paralyzed Fingers: A Case Series in Chronic and Acute Stroke Patients," *J. NeuroEng. Rehabil.* 2008, 5, 21.
- [10] L. Dovat, O. Lambercy, R. Gassert, T. Maeder, T. Milner, T.C. Leong and E. Burdet, "HandCARE: A Cable-Actuated Rehabilitation System to Train Hand Function after Stroke," *IEEE Trans. Neural Syst. Rehabil. Eng.* 2008, 16, 582–591.
- [11] H.M. Qassim and W.Z. Wan Hasan, "A Review on Upper Limb Rehabilitation Robots," *Appl. Sci.* 10, 6976. Oct 2020.
- [12] J. McNamara, "What Design Engineers Need to Know About VCA (Voice Coil Actuator) Technology," *Sensata Technologies*, White Paper, Jun 2018 [Online]. Available: <https://www.sensata.com/resources/white-paper-what-design-engineers-need-know-about-vca-voice-coil-actuator-technology>
- [13] S. Kang, YG. Jeong and YM. Choi, "Design of a Finger-Sized Voice Coil Motor for High-Speed Scanners," *Int. J. Precis. Eng. Manuf.* 24, 209–217, Dec 2022.
- [14] VC250/M - Voice Coil Actuator Spec Sheet [Online]. Available: <https://www.thorlabs.com/thorproduct.cfm?partnumber=VC250/M>